

# Mass-spectrometric investigation of the neutral particles of a laser plasma

Yu. A. Bykovskii, S. M. Sil'nov, E. A. Sotnichenko, and B. A. Shestakov

Moscow Engineering-Physics Institute

(Submitted 5 June 1986)

Zh. Eksp. Teor. Fiz. **93**, 500–508 (August 1987)

The physical processes ensuing from interaction of laser radiation with matter are investigated. The results of experimental investigations of the plasma neutral component produced when picosecond radiation acts on a solid target are reported. Preionized atomic beams are analyzed with time-of-flight mass-spectrometry methods. The energy, velocity, and angular distribution of the atoms are investigated, the integrated characteristics of the neutral beams are obtained, and the mechanisms responsible for the energy spectra of the atoms in a radiation intensity interval  $q = 10^7\text{--}10^{10}$  W/cm<sup>2</sup> are described over the broad mass range from carbon to lead.

Recent measurements have shown that a plasma produced by a  $Q$ -switched laser is a powerful source of particles of all kinds, including neutrals. The properties of laser plasmas were exhaustively investigated with the aim of developing particle sources for accelerators and mass spectrometers, producing controlled thermonuclear power, etc. The ion component of a laser plasma is analyzed most frequently by time-of-flight mass-spectrometry. The energy, charge, and angular distribution of singly and multiply ionized atomic and molecular ions are investigated<sup>1–3</sup> in a wide range of laser-beam intensities and for a large class of materials. Little attention was paid earlier to the neutral component, which contains, however, abundant information on the physical processes involved in the production and development of a plasma blob. Analysis of the energy and velocity distribution of the atoms, of the mutual influence of the charged and neutral particle streams, and of the interpretation of the ionization and recombination processes plays an important role even for very high radiation intensities. The use of streams of neutral atoms from a laser-induced plasma as sources of atoms for charged-particle accelerators<sup>4</sup> is relevant for the development of various devices that feed the working medium into various discharge gaps of electrophysical devices, for implementing methods of depositing thin films by lasers,<sup>5</sup> and for other applications.

Our purpose was to investigate the mechanism whereby the neutral component of a laser plasma is produced, and to study the energy, velocity, and global characteristics of the atom fluxes.

Atomic beams were recorded by ionizing the atoms by various methods based on the use of a laser plasma as a source of particles that ionize the investigated atoms and permit analysis of the resulting ions. Neutral particles are mass- and velocity-analyzed by time-of-flight mass-spec-

trometry procedure. The experimental setup, the atom-diagnostics system, and the measurement procedure are described in detail in Refs. 6–8. The diagnostic-system sensitivity thresholds are estimated to be atomic density  $10^8\text{--}10^9$  cm<sup>-3</sup>, atom flux  $10^{12}$  at/min, and minimum recorded-particle energy 0.5 eV. The radiation sources were electro-optically  $Q$ -switched lasers delivering 60 mJ in a 10-ns pulse at a wavelength  $\lambda = 10.6$   $\mu$ m in an intensity interval  $10^7\text{--}10^{10}$  W/cm<sup>2</sup>.

## 1. EVAPORATION PROCESSES

The processes involved in metal evaporation by nanosecond laser pulses at low radiation intensities have been investigated relatively little. The surface layer of the sample is evaporated when the incident radiation exceeds a limiting value  $q \geq q_1$ . The limiting values of  $q_1$  of various materials are gathered in Table I and differ significantly from the data for longer millisecond pulses, for which  $q_1 = 10^5\text{--}10^6$  W/cm<sup>2</sup>.<sup>9</sup> The radiation intensities that characterize the disintegration of the sample surface are several times lower than the analogous ones determined earlier by measuring the ion component of the plasma.

The energy distributions of the atoms obtained by evaporating carbon, aluminum, cobalt, cadmium, and lead samples are shown, for the corresponding limiting values  $q_1$ , in Fig. 1a:

- 1) the energy spectra have a regular shape (almost symmetric about the intensity maximum);
- 2) the energy spectra of the particles broaden monotonically with atomic number and their intensity maxima shift towards higher energies;
- 3) the atomic beam has a different energy limit for each substance;

TABLE I. Parameters of atom fluxes at laser-emission intensity limit.

Target Material	$q_1, 10^7$ W/cm <sup>2</sup>	$N_{at}, 10^{12}$	$E_m^{exp}, eV$	$E_0^{calc}, eV$	$v_m^{exp}, 10^8$ cm/s	$v_0^{calc}, 10^8$ cm/s	$u_m, 10^8$ cm/s	$kT_a, eV$
C	8	3.2	2	0.3	5.8	2.4	4.3	0.25
Al	10	1.6	5	0.7	5.8	2.3	4.8	0.68
Co	8	1.6	8	1.1	5.0	1.9	4.8	1.5
Cd	2	2.1	18	2.8	5.9	2.2	4.5	2.5
Pb	1	3.3	21	3.8	4.5	1.9	3.5	2.9

Note.  $E_m^{exp}$  and  $v_m^{exp}$  are the measured atom energies and velocities at the peaks of the spectra;  $E_0^{calc}$  and  $v_0^{calc}$  are the energy and velocity of the directed motion, determined from the Maxwellian distribution function;  $kT_a$  is the plasma temperature and  $u_m$  is the gasdynamic expansion rate.

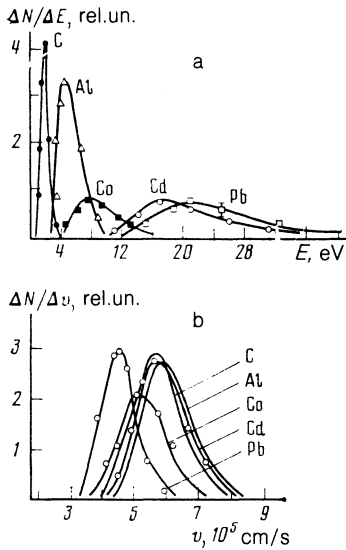


FIG. 1. Energy (a) and velocity (b) spectra of C, Al, Co, Cd, and Pb atoms at "limiting" laser-emission intensities  $q_1$  and at  $d = 1$  mm (light circles—Maxwellian distribution functions).

4) the atom energies range from 0.5–4 eV for carbon to 12–40 eV for lead.

The atom velocities are  $(3-8) \cdot 10^5$  cm/s and differ insignificantly at the distribution maxima;  $v_m^{\text{exp}} = (5-6) \cdot 10^5$  cm/s for all investigated materials.

The low values of  $q_1$  and the shapes of the spectra indicate that these atomic beams are produced by thermal evaporation. To determine the possible temperature of a beam, and the energy and the directed velocity of the atoms, we investigated the shapes of the particle velocity distributions by comparing the experimentally obtained atom spectra with the Maxwellian distribution function. The procedure developed in Ref. 10 yielded for a Maxwellian distribution the following relations for the number  $dN_a/dE$  of neutral particles recorded by the analyzer per unit energy interval, the temperature  $T_a$ , and the directed motion energy  $E_0$ :

$$\frac{dN_a}{dE} = \frac{2\pi}{M^2} n_a \left( \frac{M}{2\pi kT_a} \right)^{3/2} (E - e\varphi) \times \exp \left\{ - \frac{[(E - e\varphi)^{1/2} - E_0^{1/2}]^2}{kT_a} \right\} S\tau\Delta\Omega,$$

$$kT_a = (E_m - e\varphi)(1 - b^{1/2}), \quad E_0 = (E_m - e\varphi)b,$$

where  $M$  is the atom mass,  $n_a$  the atom density,  $\varphi$  the gasdynamic "plasma potential,"  $E_m$  the energy at the maximum of the distribution,  $S$  the cross section area of the entrance diaphragm of the analyzer,  $\tau$  the duration of the atom stream,  $\Omega$  a solid angle determined by the geometry of the analyzer, and the coefficients  $e\varphi$  and  $b$  are appropriately defined in Ref. 10.

The result of the comparison of the Maxwellian distribution function (light circles) with the experimentally obtained one is shown in Fig. 1b and demonstrates the satisfactory agreement between these relations; this undoubtedly confirms the thermal origin of the atom formation. The experimentally obtained energy and velocity characteristics of the atomic beams and the parameters determined from the Maxwellian function at threshold intensity are summarized in Table I. The maximum values of the gasdynamic atom

expansion velocities were calculated from an equation of Ref. 11 and are also listed in Table I:

$$u_m = \frac{2}{1-\gamma} v_s, \quad v_s = 10^6 \left( \frac{kT_a}{A} \right)^{1/2} \text{ cm/s};$$

here  $v_s$  is the speed of sound in the stream for the  $T_a$  obtained for  $\gamma = 5/3$ . The fact that the neutral particles have directed velocities that are high compared with the thermal velocity and are practically independent of the atomic weights of the particles is evidence of gas-dynamic acceleration of the atom bunches as they spread out into the vacuum. The velocity distributions for elements with different atomic weights cannot be approximated by a Maxwellian function with a single parameter  $T_a$ , and the temperature of the neutral blob increases with target atomic number.

We consider how the energy spectra of the atoms develop as the laser-emission intensity increases, using as an example the cobalt sample results shown in Fig. 2a. In the range  $(8-16) \cdot 10^7$  W/cm<sup>2</sup> the number of thermal particles increases without a substantial change of the spectrum shape as the energy interval of the atoms broadens in the range 2–20 eV, while the maximum of the distribution shifts by 5–10 eV. As  $q$  increases, the atom velocities (at the distribution peak) increase from  $6 \cdot 10^5$  to  $11 \cdot 10^5$  cm/s in proportion to  $q^{1/4}$ . The integrated yield of the neutral fluxes varies in the range  $(1-60) \cdot 10^{12}$  at/pulse, depending on the laser-emission intensity and on the sample material (see Fig. 4 below)

## 2. INFLUENCE OF RECOMBINATION ON THE FORMATION OF THE ATOM SPECTRA

A distinctive feature in the distributions of the atoms of all elements as the incident-radiation energy increases is that at a certain limiting value of  $q_2$  the spectrum acquires a second intensity maximum, and a group of particles appears in the region of higher energies. The values of the "secondary limiting" radiation intensities  $q_2$  are listed in Table II. The appearance of a group of high-energy particles ( $E > 40$  eV) in the neutral blob attests to a start of a recombination process, with a correlation established between the  $q_2$  and  $I_i$  (the ionization potential), and also between  $q_2$  and  $E_b + I_i$  (the sum of the binding energy of the atom in the lattice and

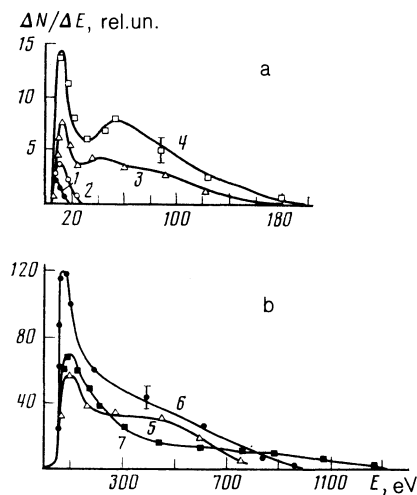


FIG. 2. Energy distributions of Co atoms at  $d = 300 \mu\text{m}$ : a) 1 –  $q = 9 \cdot 10^7$  W/cm<sup>2</sup>, 2 –  $1 \cdot 10^8$  W/cm<sup>2</sup>, 3 –  $2 \cdot 10^8$  W/cm<sup>2</sup>, 4 –  $3 \cdot 10^8$  W/cm<sup>2</sup>; b) 5 –  $q = 2.5 \cdot 10^9$  W/cm<sup>2</sup>, 6 –  $3.5 \cdot 10^9$  W/cm<sup>2</sup>. 7 –  $5 \cdot 10^9$  W/cm<sup>2</sup>.

TABLE II. Second limiting intensities of the laser radiation.

Target material	$q_2$ , W/cm <sup>2</sup>	$I_i$ , eV	$E_b + I_i$ , eV
Pb	$1 \cdot 10^8$	7.4	9.4
Al	$1.5 \cdot 10^8$	5.9	9.2
Cd	$2 \cdot 10^8$	7.7	11
Co	$2 \cdot 10^8$	7.9	12.1
C	$5 \cdot 10^8$	11.3	14.9

Note.  $I_i$  is the first ionization potential;  $E_b$  is the atomic binding energy.

the ionization potential. This, in turn, is evidence of the onset ionization and formation of a laser plasma, a process characterized by quantities  $q_2$  which are lower than the analogous values determined by measuring the ion component of the plasma.<sup>2</sup>

We turn now to the cobalt-atom energy spectra shown in Fig. 2. When the laser radiation intensity reaches  $2 \cdot 10^8$  W/cm<sup>2</sup> atoms appear in the blob with energies up to 200 eV, gathered into a second particle-intensity maximum in the vicinity of 40 eV (Fig. 2a). This is followed by division of the spectrum into two parts, with energies 10 and 60 eV at the maxima. In the  $(4-10) \cdot 10^8$  W/cm<sup>2</sup> band, the number of atoms in the plasma continues to increase strongly as the energies of the atoms in the beams increase to 700 eV, the amplitude of the maximum of the energy spectrum increases from  $E = 60$  eV compared with the low-energy maximum, a single maximum develops in the atom distributions at  $E = 60$  eV, and groups of neutral particles appear with energies  $\sim 200$  and 400 eV at the maxima. As  $q$  increases further in the interval  $(1-5) \cdot 10^9$  W/cm<sup>2</sup> (Fig. 2b), the growth of the spectrum amplitudes slows down, the principal maximum shifts to the region (75-100) eV, and atoms with energies up to 1 keV are recorded. Above  $q \geq (5-7) \cdot 10^9$  W/cm<sup>2</sup> the number of neutral particles in the plasma begins to decrease, and atoms with energies up to 1.5 keV appear in the spectrum. Similar dynamics was verified for the development of the energy distributions of the atoms of all the materials investigated.

It has thus been established by experiment that when the limiting energy of the incident radiation is reached, the sample begins to evaporate intensively and, as the radiation flux density increases further to the "second limiting" values, ionization of the evaporated matter begins, fast recombination streams of the atoms appear, and a laser-induced plasma is produced.

Analysis of the energy and velocity spectra of atoms of various elements and of the way they depend on the incident radiation show that recombination strongly influences the formation of the neutral component of a laser plasma. It is therefore most convenient to track the evolution of the plasma by comparing the energy spectra of the atoms with the energy and charge spectra of the ions in a set of experiments on manganese.<sup>1</sup> At  $q = 1.1 \cdot 10^8$  W/cm<sup>2</sup> only singly charged ions are produced in the energy interval 25-75 eV, with a spectrum maximum at  $E = 55$  eV; in this case the atom-energy range is 2-60 eV, and the maximum is in the region of  $E = 20$  eV. When singly and doubly charged ions appear with energies 100-200 eV, the atom spectrum broadens to 150 eV ( $q = 3 \cdot 10^8$  W/cm<sup>2</sup>) and a second maximum of the neutral particle intensity, due to recombination of singly charged ions, is registered at  $E = 50$  eV. With further increase of the laser-emission intensity, ions with higher

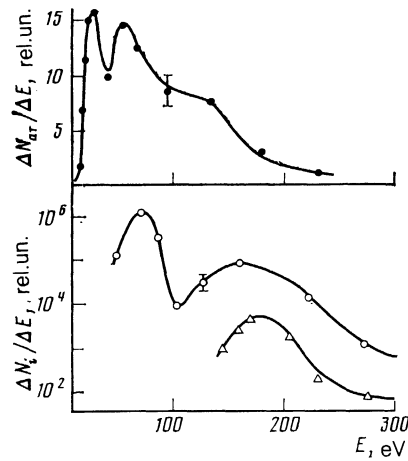


FIG. 3. Energy spectra of atoms (top) and ions (bottom) of a laser-induced magnesium plasma for  $q = 4 \cdot 10^8$  W/cm<sup>2</sup>.

charges are produced and contribute to the distribution in energies with  $z = +2$ ,  $z = +1$  and  $z = 0$  (see Fig. 3). When  $q$  increases to  $5.5 \cdot 10^8$  and  $1 \cdot 10^9$  W/cm<sup>2</sup>, the total number of the high-energy neutral particles continues to grow, the atom energies increase to 350 and 600 eV, respectively, and the ion energies to 400 and 800 eV. A decrease and shift of the first recombination maximum to the region 70-90 eV takes place in the distribution of the atoms, and pronounced maxima of the particle intensities in the high energy region (230 and 350 eV) appear on the spectra. Consequently, the intensity maxima that appear in the atom spectra near energies typical of the ion component of the laser plasma are produced by recombination of the ions with  $z = +1$ ,  $z = +2$ , and  $z = +3$ , and the distributions of the atoms duplicate the bell shape typical of ions. A comparative analysis of the distributions of the neutral and charged components of a laser plasma reveals the following main patterns:

- 1) on the whole, the energy ranges of the ions and atoms are the same;
- 2) the limiting energies in atom spectra are lower than for ions, and the difference between the right-hand boundaries of the ion and atom distributions increases with increase of  $q$ ; this is due to the "quenching" of the multiply charged ions on the periphery of the plasma flare;
- 3) the maxima of the particle intensities in the atom spectra are shifted towards lower energies relative to the maxima of the ion distributions.

The distribution of the neutral particles in energy depends substantially on the initial dimension  $d$  of the plasma blob, and the role of the recombination process increases with increasing  $d$ .<sup>12</sup> The energy spectra of manganese atoms, obtained at different  $d = 300-900$   $\mu$ m but at equal irradiation intensities, show that:

- 1) as  $d$  increases the maximum of the energy spectrum broadens noticeably and shifts towards higher energies;
- 2) in view of the appearance of high-energy particles, the absolute yield of atoms increases with  $d$ ;
- 3) the energy distribution changes shape mainly in the recombination part of the spectrum.

The energy spectra of the neutral particles of a laser plasma with  $E > 40$  eV are thus determined exclusively by recombination processes, yielding direct information on the recombination.

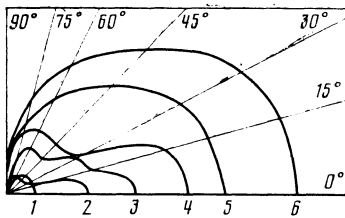


FIG. 4. Dispersal of Co atoms in angle: 1 -  $q = 1.9 \cdot 10^8$  W/cm<sup>2</sup>; 2 -  $2.4 \cdot 10^8$  W/cm<sup>2</sup>; 3 -  $5.3 \cdot 10^8$  W/cm<sup>2</sup>; 4 -  $7 \cdot 10^8$  W/cm<sup>2</sup>; 5 -  $1.6 \cdot 10^9$  W/cm<sup>2</sup>; 6 -  $4 \cdot 10^9$  W/cm<sup>2</sup>.

### 3. ANGULAR DISPERSAL OF ATOMS

A feature of the angular dispersal of the atoms at threshold intensities of the incident radiation  $q$ , is that the energy spectra remain practically unchanged, except for the absolute yield of the neutral particles. The angular dispersal patterns at radiation intensities  $1 \cdot 10^8$ – $5 \cdot 10^9$  W/cm<sup>2</sup> are shown in Fig. 4.

Analysis of the energy spectra and of the atoms at various dispersal angles with increase of  $q$ , and of the dispersal diagrams, has shown the following:

1) the angular distributions and the dispersal diagrams of the atoms stretch out along the normal to the sample and as  $q$  increases they broaden significantly because the appearance of a large number of recombination atoms in the solid angle  $\Omega \leq 45^\circ$ ;

2) the emission angle of the high-energy atoms increases monotonically with  $q$ ;

3) the recombination atoms have the narrowest angular distribution at the instant they appear in the plasma blob at intensities  $q_2$ ;

4) as the angle between the atom emission from the plasma blob and the normal to the sample is decreased, the maximum (limiting) energies of the recorded atoms increase, broaden, and shift towards higher energies;

5) the neutral component disperses into larger angles with the normal to the sample ( $\Omega \geq 60^\circ$ ) compared with the ion component.

### 4. QUANTITATIVE PROPERTIES OF THE ATOM STREAMS

The number of atoms evaporated by the laser beam is determined to a considerable degree by the thermophysical properties of the samples. Table III lists the atomic yields of the investigated materials at  $q = 4 \cdot 10^8$  W/cm<sup>2</sup> as function of the atom binding energy in the crystal lattice and of the parameter  $I_i/kT_c$  taken from Ref. 13 and equal to the ratio of the ionization potential to the critical temperature. The yield of lead and cadmium atoms can exceed that of the other elements by a factor of ten, owing to the low binding energy and evaporation temperature, so that most laser energy is used to increase the total number of evaporated atoms.

The measured number of thermal and recombination

atoms, and the charged component, are shown for a cobalt plasma as functions of the emission laser intensity in Fig. 5. As the radiation intensity increases in the plasma, but at higher values an appreciable fraction of the radiation energy goes to heat the plasma and to increase the average charge of the ions and the translational energy. The thermal-atom yield predominates only in the narrow radiation-intensity interval  $(8-30) \cdot 10^7$  W/cm<sup>2</sup>, i.e., between the first and second limiting values, and reaches a maximum emission when strong screening of the radiation by the evaporated matter sets in. In the range  $(3-6) \cdot 10^8$  W/cm<sup>2</sup> the number of recombination atoms is several times larger than the number of atoms of thermal origin, and becomes more than 10–100 times larger starting with  $q \geq 6 \cdot 10^8$  W/cm<sup>2</sup>. Experiment has shown that in the emission intensity range  $10^8$ – $10^{10}$  W/cm<sup>2</sup> the charged component is 0.4 to 5% of the total number of laser-plasma particles for a large number of materials.

These totals show that more than 95% of the particles in an expanding laser-induced plasma blob are neutral and constitute recombined atoms.

### CONCLUSION

We have reported the results of a set of experiments on the neutral plasma component produced by irradiating a solid target with nanosecond laser pulses. We used a time-of-flight spectrometer with preliminary ionization of the investigated atom streams. We studied in detail the energy, velocity, and angular distributions of the atoms and the integral characteristics of the neutral streams, and described the dynamics of the atom energy spectra in the radiation-intensity interval  $10^7$ – $10^{10}$  W/cm<sup>2</sup>, for elements in the wide mass range from carbon to lead.

The energy spectrum of the laser-induced plasma atoms was found to have a complex structure, consisting of a low-energy part with atom energies from 0.5 to 40 eV, and a high-energy part from 40 eV to 1.5 keV. It was established that the formation of high-energy atom beams is due entirely to recombination processes, and the atomic distribution in the low-energy region is determined by thermal and secondary mechanisms.

Intense thermal evaporation of the sample material sets in at a certain threshold radiation energy. When higher (second) threshold energy values are reached, ionization of the evaporated cloud begins, a laser-induced plasma is produced, and recombination-atom streams appear. Up to  $q = 5 \cdot 10^9$  W/cm<sup>2</sup> the radiation energy mainly increases the number of both the neutral and the charged particles in the plasma, but at higher  $q$  values an appreciable fraction of the energy goes to plasma heating, to increase of the average charge of the ion component, and to increase of the translational energies of the atoms and ions.

A comparative analysis of the charged and neutral com-

TABLE III. Atomic yield from various targets at  $q = 4 \cdot 10^8$  W/cm<sup>2</sup>.

	Target material			
	Ti	Al	Pb	Cd
$N$ , at/pulse	$1 \cdot 10^{13}$	$3 \cdot 10^{13}$	$5 \cdot 10^{14}$	$7 \cdot 10^{14}$
$E_b$ , eV	4.8	3.3	2.04	1.16
$I_i/kT_c$	6.7	8.6	17.3	37.1

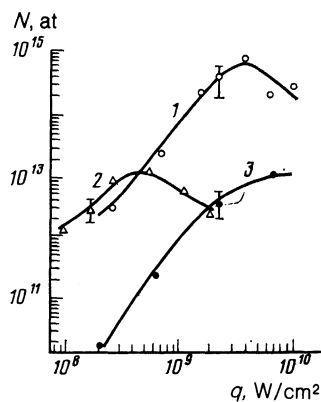


FIG. 5. Yield of laser-induced Co-plasma particles vs the emission intensities of the recombination atoms (1), thermal atoms (2), and ions (3).

ponents of the laser-produced plasma attests to the decisive role played by the recombination in the dispersal of the atomic particles and leads to the conclusion that more than 95% of the plasma consists (depending on the radiation intensity) of neutral particles, the bulk of the latter being recombined atoms.

The study of the physical characteristics of the neutral component of the laser component of the laser plasma, such as the density, duration, and velocity of the atom streams leads to specific recommendations concerning the use of a laser-induced plasmoid as a source of neutral particles for

electrophysical and nuclear-physical apparatus<sup>14</sup> and for industry.

- <sup>1</sup>Yu. A. Bykovskii, N. N. Degtyarev, N. N. Elesin, Yu. P. Kozyrev, and S. M. Sil'nov, *Zh. Eksp. Teor. Fiz.* **60**, 1306 (1971) [*Sov. Phys. JETP* **33**, 706 (1971)].
- <sup>2</sup>G. M. Arukhanyan, D. D. Bogdanov, Yu. A. Bykovskii, *et al.*, JINR Preprint R7-82-749, Dubna, 1982.
- <sup>3</sup>V. V. Berezovskii, Yu. A. Bykovskii, *et al.*, *Pis'ma Zh. Tekh. Fiz.* **3**, 310 (1977) [*Sov. J. Tech. Phys. Lett.* **3**, 126 (1977)].
- <sup>4</sup>Yu. A. Bykovskii, V. E. Mironov, V. P. Sarantsev, *et al.*, *Zh. Tekh. Fiz.* **54**, 527 (1981) [*Sov. Phys. Tech. Phys.* **29**, 313 (1981)].
- <sup>5</sup>Yu. A. Bykovskii, A. G. Dodoladov, L. K. Kovalev, *et al.*, Proc. 7th All-Union Conf. on the Interaction of Atomic Particles with Solids, Minsk, 1984, p. 273.
- <sup>6</sup>Yu. A. Bykovskii, V. E. Mironov, V. P. Sarantsev, *et al.*, JINR Preprint R13-83-807, Dubna, 1983.
- <sup>7</sup>Yu. A. Bykovskii, V. E. Mironov, V. P. Sarantsev, *et al.*, JINR Preprint 13-83-807, Dubna, 1983.
- <sup>8</sup>Yu. A. Bykovskii, V. E. Mironov, V. P. Sarantsev, *et al.*, Sov. Patent No. 1127460, Byull. "Otkrytiya, izobreteniya," (Patent Disclosure Bulletin) No. 20, 244 (1985).
- <sup>9</sup>V. A. Batanov, F. V. Bunkin, A. M. Prokhorov, and V. B. Fedorov, *Zh. Eksp. Teor. Fiz.* **63**, 586 (1972) [*Sov. Phys. JETP* **36**, 311 (1973)].
- <sup>10</sup>A. G. Tolostolutskiĭ, I. N. Zolototubov, Yu. M. Novikov, and I. P. Skoblik, Kharkov Physicotech. Inst. Preprint No. 70, 1973.
- <sup>11</sup>Ya. B. Zel'dovich and Yu. P. Raizer, *Physics of Shock Waves and High-Temperature Phenomena*, Academic, New York (1966, 1967).
- <sup>12</sup>Yu. A. Bykovskii, S. M. Sil'nov, B. Yu. Sharkov, S. M. Shuvalov, and G. A. Sheroziya, *Fiz. Plasmy* **2**, 248 (1976) [*Sov. J. Plasma Phys.* **2**, 136 (1976)].
- <sup>13</sup>V. I. Luchin, *Izv. Vysshch. Ucheb. Zaved.* **23**, 177 (1980).
- <sup>14</sup>V. T. Mironov, S. M. Sil'nov, E. A. Sotnichenko, and B. A. Shestakov, JINR Preprint 9-83-837, Dubna, 1983.

Translated by J. Adashko